HEFAT2014
10th International Conference on Heat Transfer, Fluid Mechanics and Thermodynamics
14 – 16 July 2014
Orlando, Florida

WAVY RIBBON FORMATION DURING PLANAR FLOW MELT SPINNING PROCESS – A 3D CFD ANALYSIS

Sowjanya M.[1,2] and Kishen Kumar Tadisina Reddy [2,*]
[*]Author for correspondence
[1]*Muffakham Jah College of Engineering and Technology, Hyderabad-500034, India*
[2]*Jawaharlal Nehru Technological University, Hyderabad-500085, India*
E-mail: reddykishen@jntuh.ac.in.

ABSTRACT

Planar flow melt spinning is a rapid solidification process used to produce amorphous ribbons for transformer core applications, etc. Molten metal is ejected via a nozzle onto a rotating cooling wheel for rapid solidification which bypasses crystallization. The study of surface feature (topography) is a measure of surface quality of the ribbon obtained. Experiments often result in formation of amorphous ribbons with different surface topographies such as wavy, dimple, herringbone, streak, etc which are imperfections, leading to non-uniform magnetic properties. An amorphous ribbon of polished surface topography is preferred for better performance of the magnetic core in the transformers. Hence to understand this phenomenon, a 3D numerical simulation of ribbon formation is performed to predict the ribbon surface. The computational domain consists of the space between the nozzle (from which the molten metal issues) and the rotating cooling wheel on which the molten metal falls, solidifies instantly and forms an amorphous strip. The Computational domain is extended on both sides of the nozzle to include the surrounding atmosphere. The solid cooling wheel is modeled as a curved wall boundary at constant temperature. A CFD technique called volume of fluid is used to simulate the two phase flow of melt in the air domain over the wheel surface. The conservation equations of Mass, Energy and Momentum are solved under transient conditions. Temperature dependent viscosity relation is used for the melt to employ the viscous changes in the ribbon flow. For a set of process conditions, wavy ribbon pattern is observed at lower melt ejection temperatures. By increasing the ejection temperature keeping other process conditions constant, polished ribbon is obtained. Upstream meniscus is observed to play an important role in the surface topography of the ribbon. Topographical changes in the ribbon are due to momentum transport mechanism during melt flow, which in turn depends on the surface tension and temperature dependent viscosity. Hence, a variation in ejection temperature leads to changes in surface topography of the ribbons. 3D model and simulations presented in the study are useful in predicting the surface topography of the ribbon for a set of process conditions selected for experimentation.

INTRODUCTION

Molten metal is ejected through a slit nozzle on to a rotating copper wheel for rapid solidification using planar flow melt spinning (PFMS) technique. A melt puddle is formed in the gap between the nozzle walls and the cooling wheel. Melt is ejected in the form of a ribbon from the undercooled puddle due to wheel rotation [1]. The cooling rate during the process cause change in viscosity in the melt puddle near to the wheel surface. Change in viscosity leads to change in momentum of the melt flow. Change in flow of melt on the quenching wheel surface leads to variation in heat transfer across the ribbon thickness. Hence the feature of the air side of the ribbon often differs to that of wheel side. The surface feature of the ribbon is a measure of its quality. Uneven surfaces may result in uneven magnetic properties. Hence the study of surface feature (topography) of the ribbon formed during PFMS process is of interest to produce quality product. Schematic of the process is shown in Fig. 1(a) and ribbons of various topographies are presented in Fig. 1(b). Polished ribbon is preferred for the end use as a magnetic core in the transformer over other ribbons with surface features like dimple, wavy, herringbone, streak etc., obtained during experiments [2-4 and 9]. At high Stephan numbers dimple pattern was observed [2]. Non uniform flow of melt was observed to result in herringbone pattern [3]. Imperfect contact between ribbon and wheel led to streak pattern and wave pattern due to unstable meniscus [8]. Few numerical investigators, assumed constant value for the contact angle between the melt puddle and the wheel [6, 7]. In the present study this was calculated based on the process conditions. Present authors simulated puddle formation (Fig. 2(a)) in 2D and compared with high speed image (Fig. 2(b)) taken during experiment conducted at the same process conditions [10]. A 3D model is developed to find the surface topography of the ribbon obtained during experiments [11]. In the present study this model is used to predict and analyse the conditions at which a wavy ribbon is obtained. The model can be used to predict the surface topography of a ribbon for a set of process conditions before execution of the experiment.

NOMENCLATURE

F	[-]	volume fraction
P	[kPa]	ejection pressure
V	[m/s]	wheel speed
T	[K]	ejection temperature
T_g	[K]	glass transition temperature
C_p	[J/kg K]	specific heat
ρ	[kg/m^3]	density
μ	[Pa. s]	dynamic viscosity
k	W/m K	thermal conductivity
g	[m/s^2]	gravitational acceleration
σ	[N/m]	surface tension

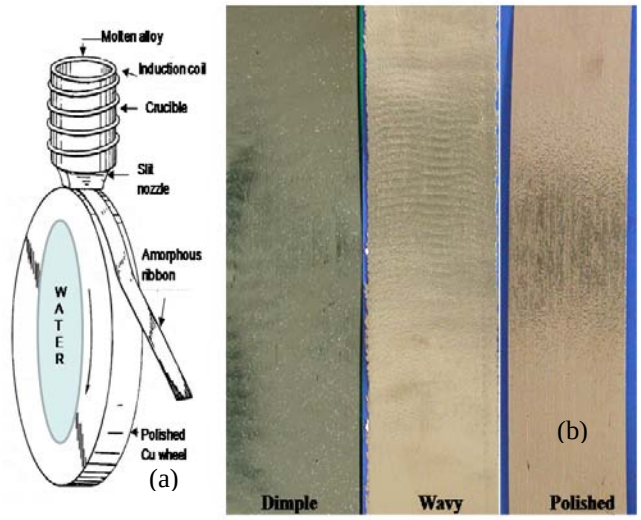

Figure 1 Schematic of (a) Melt spinning process (b) Ribbons with various topographies

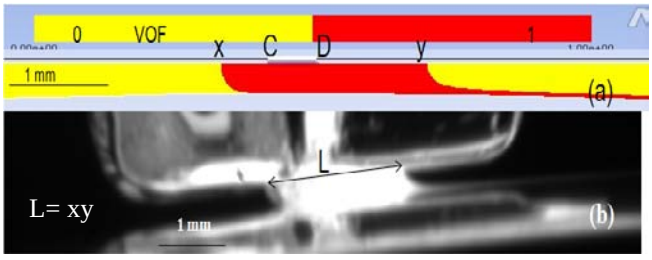

Figure 2 (a) 2D simulation of puddle formation. (b) High speed image of the puddle formed at process conditions at P=9.8kPa, w: 0.5 mm, V: 17 m/s, G: 0.2 mm and T= 1100 ^oC [10].

NUMERICAL MODEL

In the 2D model [10] shown in Fig. 2(a) melt contact length 'xy' at the nozzle is observed to be nearly equal to the length 'L' measured from the high speed image shown in Fig. 2(b). The model is extended in the z-axis direction to capture the melt flow over the wheel surface. Fig. 3(a) shows the high speed image of the melt puddle formed during experiments. Space between nozzle walls and rotating copper wheel is taken as the computational domain extending on both sides of the nozzle to include the surrounding atmosphere. Surfaces A1,A2 and A3 denote surrounding atmosphere, surface N represent nozzle walls on both sides of melt inlet MI. Surface OS represents outlet of the domain and surface S represents a part of moving wheel. 3D domain generated using ICEM CFD is presented in Fig. 3(b). A high quality (0.9) quad mesh was generated for the simulations. Conservation equations were solved under transient conditions and volume of fluid technique is used to simulate the two phase flow. Domain is assumed to be filled initially with air. Melt from the inlet enters the domain at the ejection pressure and temperature conditions. To track the free surface movement of the melt in the air domain, volume of fluid technique with geometric re-construction scheme is employed. Momentum and energy equations are solved with first order upwind scheme for the entire domain.

ASSUMPTIONS AND BOUNDARY CONDITIONS

Since amorphous ribbons are produced during PFMS process which bypasses crystallisation, the evolution of latent heat is neglected. Radiation is neglected in the simulations as most of the heat is absorbed by the copper wheel. All physical properties of melt, except viscosity are considered to be independent of temperature. Wheel surface is assumed as a perfect heat sink.

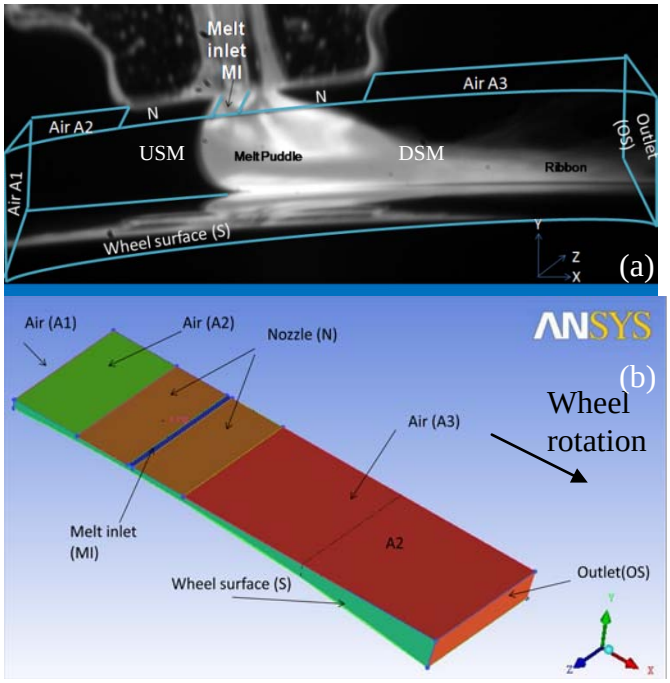

Figure 3 (a) 3D domain considered around high speed image of the puddle. (b) Numerical domain between nozzle and wheel [11].

No slip boundary condition is employed between the wheel and melt (surface S) and also between melt and nozzle walls (surface N). Wheel surface S is assumed to be smooth and at constant temperature. There is no heat flux towards the nozzle walls (N). Pressure inlet boundary is employed at melt inlet (MI) at ejection pressure. Pressure outlet condition is

employed at outlet of the domain (OS). Pressure in let condition is employed for all the air surfaces (A1, A2 and A3) at atmospheric pressure. Properties of the molten alloy used in the model (Table 1) and the equations used in the simulations are given in the appendix.

RESULTS AND DISCUSSION

Numerical simulations were carried out for the experimental process conditions at which ribbons with different topography were obtained by Majumdar et al.[9].

Ribbon formation at melt ejection temperature of 1161^{0}C

For the set of parameters P= 20.7k.Pa, V=15.7m/s, nozzle-wheel gap G=0.35mm, nozzle slit width w=0.4 mm and T= 1161^{o}C, a wavy, thick and thin ribbon of 32 μm with uneven edges was observed to obtain [9]. To capture the phenomenon of wavy ribbon formation a 3D simulation was carried out at the same process conditions.

The contact angle between melt puddle and wheel surface is calculated dynamically at given process conditions. The condition of melt and air at the upstream meniscus depends highly on the process parameters. When the melt falls on the wheel surface, surrounding air entrains at the melt wheel contact till the puddle attains stability. But puddle takes few milliseconds to stabilize on the wheel surface. Hence to capture the vibrations in the puddle which leads to wavy ribbon formation, condition of the puddle at 1.2 ms is considered. The air which enters at the bottom of the puddle also vibrates with the same frequency.

Fig. 4(a) shows the melt puddle formed between the nozzle walls and wheel surface. As ribbon formation cannot be observed in the front view, view from the top of the domain is presented in Fig. 4(b) and (c). Fig 4(b) shows the unfilled VOF contour of the melt flow over the wheel surface. AB shows the condition of the melt below the puddle, B to E shows the ribbon, ejected out of the undercooled puddle due to wheel rotation. Air bubbles in the puddle disperse in the direction of wheel rotation as shown from B to C. CD shows the transition of melt to ribbon and DE shows the solidified ribbon. The frequency of vibration is clearly shown as wavy contour in D to E. Similar trend was observed experimentally by Cormac J. Byrne et. al. and by T.J.Praisner et. al [3, 12].

Cormac et al attributed the reason for the wavy nature to the puddle oscillation due to variation in surface tension and air entrainment in the upstream meniscus (USM) side [12]. But Praisner et al reasons the wavy pattern is due to higher ejection pressure with moderate wheel speeds [3]. As the puddle vibrates with the same frequency for a set of process conditions, air bubbles enter in to the puddle continuously. The conditions at the upstream meniscus do not change throughout the cast; this trend is also repeated leading to continuous wavy nature throughout the ribbon.

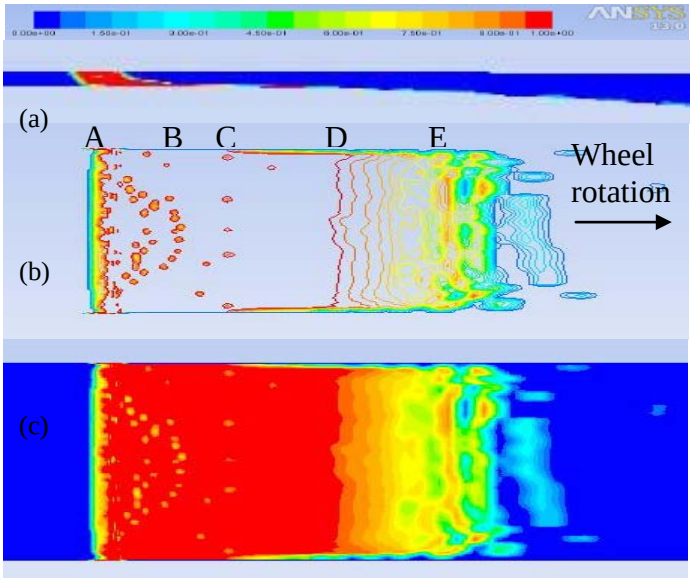

Figure 4 (a) Melt puddle formation (b) Unfilled VOF contour (c) Filled VOF contour of ribbon formation on the wheel at 1161^{o}C.

Ribbon formation at melt ejection temperature of 1500^{0}C

Fig. 5(a) shows the puddle formation and Fig. 5(b) & (c) shows the ribbon formation for a set of parameters P= 20.7 kPa, V=15.7 m/s, nozzle-wheel gap G=0.35 mm, nozzle slit width w=0.4 mm and T= 1500^{o}C for which a polished ribbon was obtained experimentally [9].

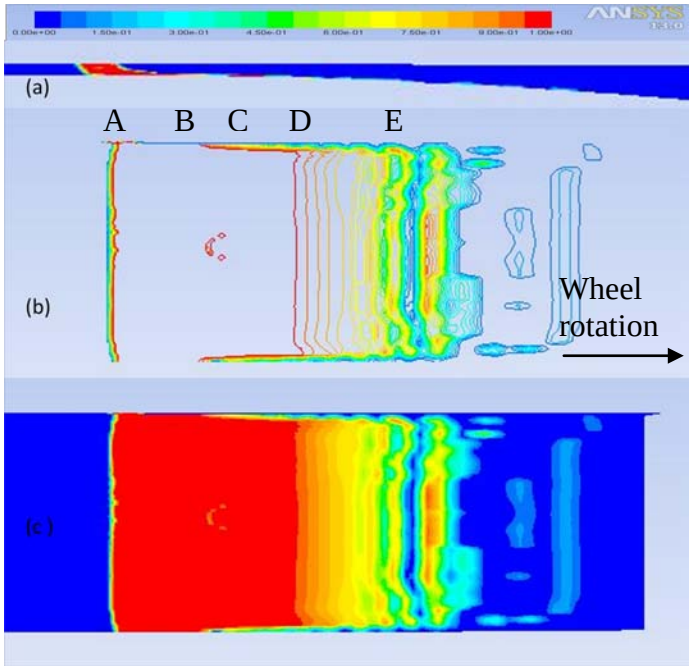

Figure 5 (a) Melt puddle formation (b) Unfilled VOF contour (c) Filled VOF contour of ribbon formation on the wheel at 1500^{o}C.

Compared to the previous case wherein wavy ribbon is obtained, the parameter that is changed is only the melt temperature from 1161^0C to 1500^0C. Lower the temperature offers more resistance to flow due to higher viscosity. This resistance contributes to oscillation in the puddle leading to wavy pattern. Oscillation in the puddle supplies molten metal from the upstream meniscus with a fixed frequency resulting in the wavy pattern of the ribbon. With increase in temperature, viscosity of the melt decreases which affects the flow ability of melt from the nozzle. Melt becomes thinner with increase in temperature and have better contact at the bottom of the puddle with the wheel. Oscillations in the puddle will be suppressed due to thinner melt in the puddle. A polished ribbon was observed by Majumdar et al. at the process conditions with ejection temperature as 1500^oC [9]. At A to D the melt is uniform and no wavy flow is observed. At DE the contours show nearly straight lines unlike in Fig. 4(b). Ribbons obtained experimentally and numerically are found to exhibit similar topography. But very high ejection temperatures lead to dimple ribbon formation which was observed experimentally [9] and presented numerically elsewhere [11].

CONCLUSIONS

Condition of the melt at upstream meniscus plays an important role in the formation of ribbon surface feature. Lower melt temperatures in planar flow melt spinning process leads to puddle oscillations due to resistance to flow at higher viscosity. The oscillations in the puddle lead to wavy ribbon. With increase in melt temperature, melt in the puddle becomes thinner due to low viscosity. Thinner melt show better spread at the melt wheel contact hence suppresses the oscillations. Wavy ribbon can be avoided by increasing the melt temperature. Simulation can be repeated for the selection of ejection temperature to get a polished ribbon when other process conditions are kept constant.

ACKNOWLEDGEMENT

Authors are thankful to Defence Metallurgical Research Laboratory (DMRL) Hyderabad, for permitting us to carry out the research work in planar flow melt spinning, to the Department of Mechanical Engineering, Jawaharlal Nehru Technological University Hyderabad for providing CFD software under DRDO Project No. ERIP/ER/1103966/M/01/1455.

APPENDIX

Table1 Properties of molten alloy used in the model.

Designation	Parameters	Values	
ρ	Density	7180 kgm^{-3}	[3]
Cp	Specific heat	544 $Jkg^{-1}K^{-1}$	[3]
K	Thermal conductivity	8.99 W/mK	[3]
μ	Viscosity	μ(T)	[6]
σ	Surface Tension	1.2 N/m	[6]

Equations used in the simulations:

Properties in the control volume cell are calculated as below:

$$\left.\begin{aligned} \rho &= \rho_m F+\rho_a (1 - F) \\ \mu &= \mu_m F+ \mu_a(1 - F) \\ C_p &= C_{p,m} F+ C_{p,a} (1 - F) \\ k &= k_m F+ k_a (1 - F) \end{aligned}\right\} \quad (1)$$

Where the suffix *'a'* denotes air and *'m'* denotes melt and F is the volume fraction of the melt in the cell.
F= 1 for melt and
F= 0 for air.

Continuity equation:

$$\partial\rho/\partial t + \partial(\rho u_i)/\partial x_i=0 \quad \text{---------- (2)}$$

Momentum equation:

$$\partial (\rho u_i)/\partial t+ \partial (\rho u_i u_j)/ \partial x_j = -\partial p/\partial x_i+ (\partial/\partial x_j) [[\mu[\partial u_i/\partial x_j +\partial u_j/\partial x_i)] +\rho g_i + f \quad \text{--- (3)}$$

Where f is the volume force term in the momentum equation resulting from surface tension, given by

$$f = (\rho k \nabla F) / [(1/2) (\rho_a+\rho_m)] \text{ and}$$

k is the curvature and given by

$$k = - \nabla[\nabla F/|\nabla F|]$$

Energy conservation equation:

$$\partial (\rho C_p T)/\partial t +\partial (\rho C_p u_i T)/ \partial x_i= (\partial/\partial x_i)(K(\partial T/\partial x_i)) \quad \text{---------- (4)}$$

Volume fraction equation:

$$(\partial F/\partial t) + u_i (\partial F/\partial x_i)= 0 \quad \text{---------- (5)}$$

Temperature dependent viscosity equation [6]

$$\mu_m = -0.1(\exp (3.6528 + 734.1/ (T - 674))) \quad \text{---------- (6)}$$

REFERENCES

1. Narasimhan, U S Patent No: 4,142,571, 1979.
2. J.K. Carpenter &P.H.Steen, Planar flow spin casting of molten metals process behavior, Journal of materials science, vol.27, 1992, pp. 215-225.
3. Thomas J. Praisner, JIM S.J.Chen, and Ampere A. Tseng, An experimental study of process behaviour in planar flow melt spinning, Metallurgical and materials transaction B, Vol. 26B, 1995,pp.1199-1208.
4. M. Srinivas, B.Majumdar, G.Phanikumar, and D.Akhtar, Effect of Planar Flow Melt Spinning Parameters on Ribbon Formation in Soft Magnetic Fe68.5Si18.5B9Nb3Cu1 Alloy, Metallurgical and materials transactions B,2011.
5. Chin – Wen Chen and Weng – Sing Hwang, A modified free surface treatment for the modeling of puddle formation in planar flow casting process, ISIJ international vol. 35, 1995, pp 393-401.
6. H. Liu, W. Chen, S. Qiu and G. Liu, Numerical Simulation of Initial Development of Fluid Flow and Heat Transfer in Planar Flow Casting Process, Metall. Mater. Trans. B, 2009, vol. 40B, pp. 411 – 429.
7. M. Bussmann, J. Mostaghimi, D.W. Kirk , J.W. Graydon, A numerical study of steady flow and temperature fields within a melt spinning puddle, Int. J.Heat and Mass Transfer,45,(2002) 3997–4010.
8. H.Yu, A fluid mechanics model of the planar flow melt spinning process under low Reynolds number conditions, Metallurgical transactions B, vol. 18B, 1987, pp. 557-563.
9. B.Majumdar, D Akhtar and V Chandrasekaran, Planar flow melt spinning of soft magnetic amorphous ribbons, Trans. Indian Inst. Met.,Vol. 60, No.2,2007,pp.343-347.
10. B. Majumdar, M. Sowjanya, M. Srinivas, D. A. Babu and T. Kishen K. Reddy, Issues on Puddle Formation During Rapid Solidification of Fe–Si–B–Nb–Cu Alloy Using Planar Flow Melt Spinning Process, Trans Indian Inst Met vol. 65 (6), December 2012, pp 841–847.
11. M. Sowjanya, T. Kishen Kumar Reddy, B. Srivathsa and B. Majumdar, Simulation of Initial Ribbon Formation during Planar Flow Melt Spinning Process, Applied Mechanics and Materials Vols. 446-447 Trans Tech Publications, Switzerland, 2014, pp 352-355.
12. Cormac.J.Byrne, Steven J.Weinstein, Paul H.Steen, Capillary stability limits for liquid metal in melt spinning, Chemical engineering science 61,2006,pp. 8004 – 8009.